Waste Technology (WasTech)
Journal homepage: http://ejournal.undip.ac.id/index.php/wastech
An International Journal

Kinetic and Isotherm Analysis of TiO_2/UiO-66-NH_2 Composites for Treating Produced Water Contaminants

Tutuk Djoko Kusworo and Budiyono

Chemical Engineering Dipoengoro University, Semarang, Indonesia
Email: tdkusworo@che.undip.ac.id

Abstract - The TiO_2/UiO-66-NH_2 composites synthesized through a hydrothermal method, demonstrated a significant enhancement in photocatalytic activity under visible light, offering a promising solution for the treatment of pollutants in produced water. These composites exhibited exceptional photocatalytic adsorption and degradation capabilities, efficiently removing various contaminants. The adsorption process during pollutant removal was effectively modeled by both the Freundlich and Langmuir isotherms, indicating the heterogeneous nature of the adsorption sites and the monolayer adsorption behavior, respectively. The composites achieved impressive removal efficiencies of 88.46% for NH_3-N and 81.97% for total dissolved solids (TDS), underscoring their potential to address common pollutants in produced water. UV-vis spectroscopy analysis revealed a band gap energy of 2.28 eV for the TiO_2/UiO-66-NH_2 composites, which is lower than that of pure TiO_2, contributing to enhanced photocatalytic performance under visible light. This reduced band gap improves the material's ability to absorb visible light, thereby facilitating more efficient degradation of organic pollutants. Furthermore, the pseudo-second-order kinetic model best described the adsorption process for both TiO_2 and TiO_2@UiO-66-NH_2 composites, suggesting that chemisorption is the dominant mechanism for NH_3-N removal. This indicates that the composites exhibit a high affinity for NH_3-N, effectively removing it from produced water. Overall, the TiO_2/UiO-66-NH_2 composites provide a promising approach for mitigating contaminants in produced water, demonstrating their potential for use in both environmental and industrial water treatment applications.

Keywords *– Produced water, TiO_2, UiO-66-NH_2, photocatalytic, adsorption.*
Doi: https://doi.org/10.14710/12.12.60-66
[How to cite this article: Kusworo, T.D. and Budiyono, (2024). Treatment of Natural Rubber Wastewater using Photoactive Nanocomposite Membrane PSf/sulfonated ZnO: Performance Evaluation, HAZOP, and Risk Analysis. Waste Technology, 12(2),60-66, doi: https://doi.org/10.14710/12.12.60-66

1. Introduction

Produced water, the largest by-product of oil and gas extraction, represents a significant environmental concern due to its complex and often toxic composition (Farnan et al., 2023). It typically contains a mixture of hydrocarbons, salts, heavy metals, radioactive materials, and a range of organic and inorganic contaminants (Zhuang et al., 2023). The improper disposal of produced water can result in severe environmental degradation, contaminating soil and water resources, and threatening both ecosystems and public health. The challenge of managing and treating produced water has thus become a focal point in addressing environmental sustainability, particularly in light of the United Nations Sustainable Development Goals (SDGs) (Obaideen et al., 2022). Specifically, SDG 6 (Clean Water and Sanitation) emphasizes the importance of ensuring clean water access, while SDG 12 (Responsible Consumption and Production) advocates for minimizing industrial waste and improving resource efficiency. Effective treatment of produced water is thus crucial for mitigating environmental risks, enhancing water recovery, and ensuring the sustainable use of water resources in industrial sectors (David et al., 2023).

Conventional methods for treating produced water, such as coagulation, adsorption, and reverse osmosis, often face limitations in terms of cost, energy consumption, and the ability to remove a broad spectrum of contaminants (César et al., 2024). In recent years, photocatalysis has emerged as a promising alternative for the treatment of wastewater, including produced water (Mishra & Sundaram, 2023). Photocatalysis offers several advantages, such as mild operational conditions, the use of sunlight as a renewable energy source, and the potential for mineralizing organic pollutants into less harmful compounds (Chakravorty & Roy, 2024). Titanium dioxide (TiO_2) is one of the most widely studied photocatalysts due to its stability, non-toxicity, and high photocatalytic activity under ultraviolet (UV) light (Pelaez et al., 2012). However, the effectiveness of TiO_2 is limited by its poor absorption in the visible light spectrum, which constitutes a significant

portion of solar energy (Etacheri et al., 2015). To address this limitation, researchers have increasingly focused on enhancing TiO_2 photocatalytic properties by integrating it with other materials, thereby expanding its light absorption range and improving its catalytic efficiency(Khan & Shah, 2023). One such material is UiO-66-NH_2, a metal-organic framework (MOF) known for its high surface area, large pore volume, and excellent adsorption capacity (Lei et al., 2023). The incorporation of amine functional groups in UiO-66-NH_2 enhances the interaction with organic contaminants, improving the overall photocatalytic degradation process (Chen et al., 2021). Furthermore, the unique structural features of MOFs, such as tunable pore sizes and the ability to create stable, highly porous composites, offer significant advantages in enhancing the photocatalytic activity of TiO_2 (Kumar et al., 2024). The combination of TiO_2 with UiO-66-NH_2 has been shown to produce composites that enhance the degradation efficiency of organic pollutants and extend light absorption into the visible spectrum, increasing their effectiveness under sunlight (Man et al., 2022).

In this context, TiO_2/UiO-66-NH_2 composites represent a highly promising approach for the treatment of produced water. The synergy between TiO_2 and UiO-66-NH_2 allows for enhanced photocatalytic performance, reduced toxicity of contaminants, and improved stability of the photocatalyst, offering a sustainable and efficient solution for water treatment. The use of TiO_2/UiO-66-NH_2 composites also aligns with the principles of circular economy and environmental sustainability by promoting the reuse of water in industrial processes and reducing the environmental footprint of oil and gas operations. This study aims to investigate the synthesis, characterization, and photocatalytic performance of TiO_2/UiO-66-NH_2 composites for the treatment of produced water, focusing on their potential to meet the growing demand for sustainable water management technologies. The findings from this research are expected to contribute significantly to advancing the development of eco-friendly and efficient water treatment methods in line with the global SDGs.

2. Materials and Methods

2.1 Materials

Zirconium chloride ($ZrCl_4$, 99.5%), titanium dioxide (TiO_2), 2-aminoterephthalic acid, methanol, acetic acid, and dimethylformamide (DMF) were obtained from Sigma-Aldrich, Singapore. HI3824-025 test kit reagents, and potassium dichromate. Deionized water was used throughout the experimental procedures to ensure purity and prevent contamination. These reagents were employed in the synthesis of materials and the subsequent preparation steps for photocatalytic experiments. The produced water sample was sourced from the Oil and Gas facility in Cirebon, West Java, Indonesia. A detailed description of the effluent characteristics is provided in Table 1.

2.2 Characterization of produced water

The preliminary analysis of the produced water focused on its physical characteristics and chemical. pH measured with a pH meter, model Y98, China, and total dissolved solids (TDS) measured with a TDS meter, model E-01, China. Chemical Oxygen Demand (COD) was determined using a UV-Vis spectrophotometer in accordance with SNI 6989.2:2019. Total Suspended Solids (TSS) were analyzed following the protocol outlined in SNI 6989.3:2019, while Biochemical Oxygen Demand (BOD) was measured as per SNI 6989.72:2009. Ammonia levels were quantified based on the guidelines of SNI 06-6989.30-2005. Table 1. shows the initial characteristics of produced water.

Table 1. Initial characteristics of produced water

No.	Parameter	Unit	Value
1	pH	-	8.3
2	TDS	ppm	4,000
3	TSS	ppm	30
4	COD	ppm	72.3
5	BOD	ppm	30.4
6	Amonia	ppm	24

2.3 Fabrication of TiO_2/UiO-66-NH_2 composite

360 mg of TiO_2 was dispersed in 60 mL of water and sonicated for 10 minutes. Then, 40 mg of MOF (to achieve 10 wt UiO-66-NH_2) was added, and the mixture was sonicated for an additional 10 minutes. The pH was adjusted, and the solution was stirred at room temperature until the solvent evaporated. The resulting powder was dried at 100 °C for 24 hours.

2.4 UV-VIS DRS analysis and adsorption studies

The optical properties of the nanofiller photocatalyst were analyzed using UV-Vis spectroscopy. The absorption spectrum was recorded over the wavelength range of 200–800 nm to evaluate the material's light absorption capabilities. A UV-Vis spectrophotometer equipped with an integrating sphere was used to ensure accurate diffuse reflectance measurements. The band gap energy (Eg) of the material was determined using the Tauc method, as represented in (Eq. 1).

$$\alpha h\nu = A\left(h\nu - E_g\right)^{n/2} \quad (1)$$

Where α, h, ν, A, and E_g represent the optical absorption coefficient, Planck's constant, photon frequency, a proportionality constant, and the band gap energy of the material, respectively. The parameter "n" is used to indicate the type of electronic transition occurring within the material, where n=1n = 1n=1 corresponds to a directly allowed transition.

2.5 Adsorption kinetics

The adsorption rate at the active sites of the TiO_2/UiO-66-NH_2 composite governs the removal of pollutants from the solution. To elucidate this process, several kinetic models were utilized, including pseudo-first-order, pseudo-

second-order, intraparticle diffusion, Elovich, mass transfer, and Bangham's models (Kusworo et al., 2024). These models provide valuable insights into the mechanisms and factors influencing pollutant adsorption, offering distinct perspectives on the process dynamics. The mathematical expressions for these models (Eq. 2-7).

$$\frac{t}{Q_t} = \frac{1}{K_2 Q_e^2} - \frac{t}{Q_e} \quad (2)$$

$$Q_t = K_{it}^{\frac{1}{2}} + C_i \quad (3)$$

$$Q_t = K_{dif} t^{1/2} + C \quad (4)$$

$$Q_t = \frac{1}{\beta}\ln(\alpha\beta) + \frac{1}{\beta}\ln t \quad (5)$$

$$\text{Ln}\,(C_0 - C_t) = \text{Ln}\,(D) - k_0.t \quad (6)$$

$$\text{Log}\,[\text{Log}\,(\frac{C_0}{C_0 - mq_t}) = \text{Log}\,(\frac{m K_b}{2.303\,V}) + \alpha\,\text{Log}\,(t) \quad (7)$$

Where Q_t and Q_e represent the pollutant adsorption capacity at a specific time and at equilibrium, respectively (both in mg/g). The parameters K_1, K_2, K_i, C_i, K, K_0, and k_b are the kinetic constants for various models, including pseudo-first-order (min^{-1}), pseudo-second-order ($g.mg^{-1}.min^{-1}$), intraparticle diffusion ($mg\ (g\ min)^{-1/2}$), Elovich ($g.mg^{-1}$), mass transfer (min^{-1}), and Bangham's model ($L.\ g^{-1}$).

2.6 Adsorption Isotherm

This study explores adsorption isotherms to understand the relationship between adsorbate quantity and its initial concentration on the TiO_2/UiO-66-NH_2 composite. The Langmuir, Freundlich, Temkin, and Dubinin-Radushkevich models (Kusworo et al., 2024) were evaluated using (Eq. 8–11).

$$\frac{1}{Q_e} = \frac{1}{K_L Q_m C_e} + \frac{1}{Q_m};\ R_L = \frac{1}{1 + K_L C_o} \quad (8)$$

$$\text{logs}\ Q_e = \text{logs}\ K_F + \frac{1}{n}\text{logs}\ C_e \quad (9)$$

$$Q_e = \frac{RT}{b_T}\ln K_T + \frac{RT}{b_T}\ln C_e \quad (10)$$

$$Q_e = q_m\, e^{-K\varepsilon 2} \quad (11)$$

Where Q_e, Q_m, C_o, and C_e represent the equilibrium and maximum adsorption capacities (mg/g), and the initial and equilibrium pollutant concentrations (mg/L), respectively. K_L, K_F, n, K_T, and b_T are the constants for the Langmuir, Freundlich, and Temkin adsorption models.

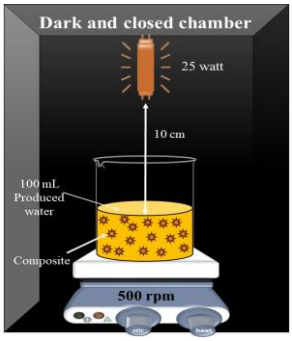

Figure 1. Illustrates the experimental setup designed for assessing photocatalytic performance.

3. Results and Discussion

3.1 UV-VIS DRS analysis

The UV-Vis spectra and Tauc plot analysis provide critical insights into the optical properties and band gap energies of various photocatalytic materials, including TiO_2, UiO-66-NH_2, and TiO_2@UiO-66-NH_2 composites. The UV-Vis spectra reveal that all three materials exhibit substantial light absorption capabilities across a broad spectral range 200–800 nm. Figure 2 presents a comprehensive analysis of the composite material's optical properties through (a) UV-Vis diffuse reflectance spectroscopy (DRS) and (b) the corresponding Tauc plot. The TiO_2@UiO-66-NH_2 photocatalyst displays a broader absorbance profile compared to pure TiO_2, indicating enhanced efficiency in utilizing visible light energy. This phenomenon is further corroborated by the red shift of the absorption edge and the reduction in band gap energy, as revealed by Tauc plot analysis. The band gap energies of TiO_2, UiO-66-NH_2, and TiO_2@UiO-66-NH_2 are determined to be 3.07 eV, 2.61 eV, and 2.28 eV, respectively. Notably, the band gap values of UiO-66-NH_2 and TiO_2@UiO-66-NH_2 are significantly lower than those of pure TiO_2 in its various crystalline forms, including anatase (3.2 eV), rutile (3.0 eV), and brookite (3.4 eV) (Sadia et al., 2024; Y. L. Wang et al., 2021)

The reduction in band gap energy suggests that these composites possess an enhanced ability to utilize visible light, which is crucial for applications under solar irradiation. This improvement can be attributed to several mechanisms. Firstly, the introduction of new energy levels within the TiO_2 band gap decreases the energy required for electronic transitions (Ye & Liang, 2024). Additionally, the TiO_2@UiO-66-NH_2 photocatalyst benefits from quantum effects arising from the reduced particle size of TiO_2 and synergistic interactions between the -NH_2 groups of UiO-66-NH_2 and TiO_2 (Monticone et al., 2000). These factors contribute to band gap reduction and improved electron transfer efficiency, effectively minimizing electron-hole pair recombination, a key factor in enhancing photocatalytic activity. The formation of composites with UiO-66-NH_2 yield materials with superior optical properties and reduced band gap energies, making them highly promising for various photocatalytic applications, including pollutant degradation and renewable energy utilization.

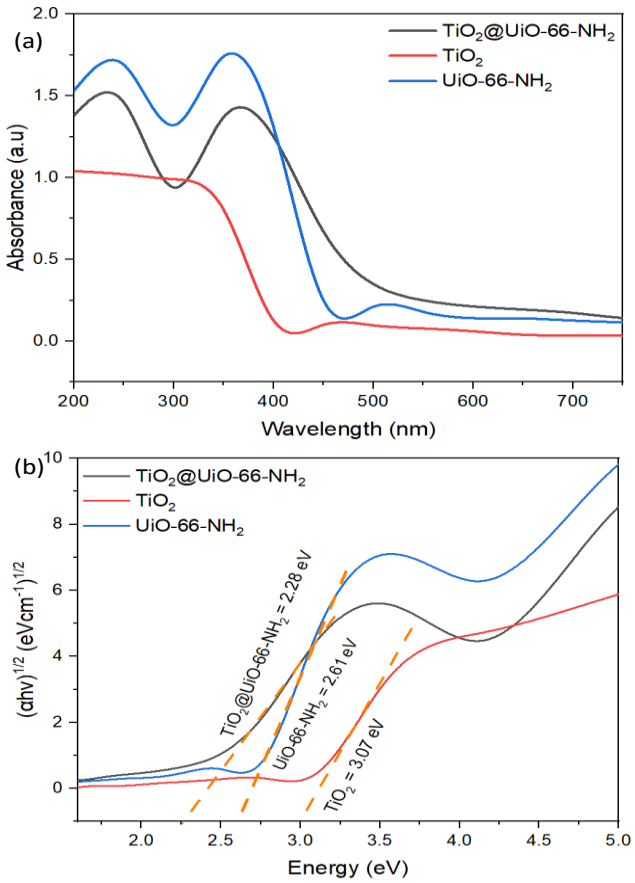

Figure 2. Analysis (a) UV-VIS DRS and (b) tauc plot of composite

3.2 Adsorption of pollutant

Figures 3(a) and (b) illustrate an increasing trend in the percentage of NH_3-N and TDS rejection with increasing contact time and catalyst dosage. Based on the analysis, a catalyst dosage of 0.3 grams was identified as the most optimal for both pollutants. This finding aligns with previous studies that highlighted catalyst dosage and contact time as two critical parameters significantly influencing the efficiency of the adsorption process (Akinyemi et al., 2024). At higher catalyst dosages, the specific surface area of the catalyst increases, offering more active sites for interaction with pollutant molecules (Sun et al., 2018). This explains the enhanced rejection efficiency observed for both NH_3-N and TDS. However, when the dosage exceeds 0.3 grams, the efficiency tends to stabilize. This reduced performance at higher dosages is likely due to catalyst agglomeration, which decreases the available surface area, or the saturation of active sites by pollutant molecules (Hachemi et al., 2024). Moreover, contact time plays a pivotal role in enhancing the rejection percentage. Pollutant molecules require adequate time to diffuse onto the catalyst surface for adsorption to occur. With sufficient contact time, adsorption efficiency continues to improve until a saturation point is reached, at which all active sites are occupied by pollutant molecules. Beyond this point, increasing the contact time has minimal to no effect on further improving efficiency, as the catalyst's adsorption capacity has already been fully utilized (Pourhakkak et al., 2021).

The observed differences in rejection patterns between NH_3-N and TDS reflect the distinct physicochemical properties of these pollutants. NH_3-N, being more polar, exhibits stronger interactions with the active sites of the catalyst, leading to higher rejection efficiency compared to TDS across all experimental conditions (C. Wang et al., 2022). In contrast, TDS, characterized by more complex physicochemical properties, may require longer contact times or additional mechanisms to achieve comparable adsorption efficiency. These findings have significant implications for the advancement of wastewater treatment technologies, particularly for produced water. By optimizing the catalyst dosage to 0.3 grams and establishing the appropriate contact time, treatment efficiency can be substantially improved without incurring excessive operational costs. Furthermore, these results underscore the potential for further exploration and development of novel photocatalysts with enhanced properties to address the challenges of treating other organic and inorganic pollutants.

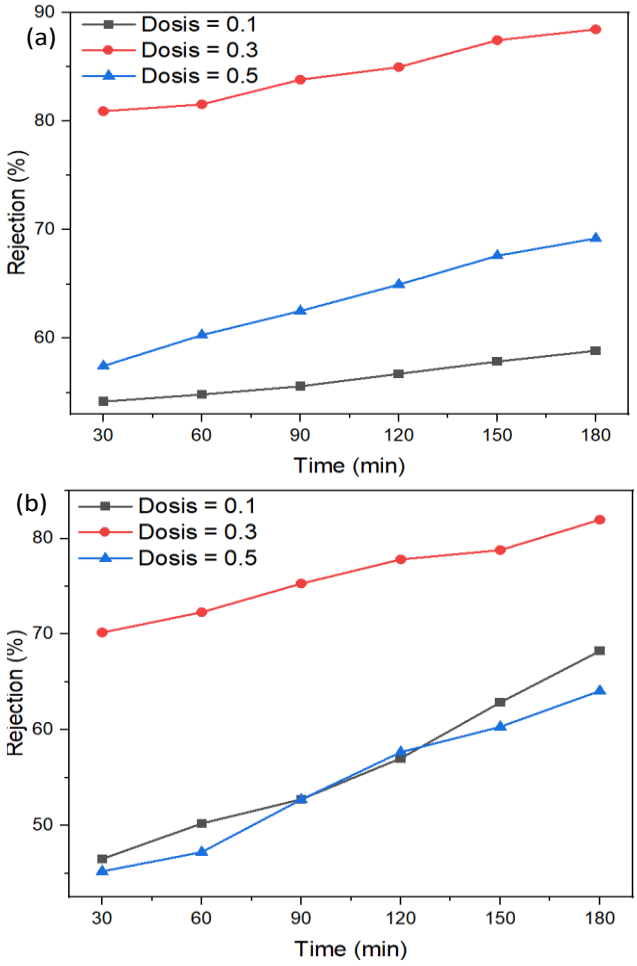

Figure 3. Effect of adsorption time and dosage on the removal of (a) NH_3-N and (b) COD at a temperature of 30°C

3.3 Adsorption Isotherm

The adsorption performance of NH_3-N on TiO_2 and TiO_2@UiO-66-NH_2 was evaluated using the Langmuir, Freundlich, Temkin, and Dubinin-Radushkevich (D-R) isotherm models, providing insights into the underlying mechanisms and efficiencies. The Langmuir model, which assumes monolayer adsorption on a homogeneous surface, revealed comparable maximum adsorption capacities (Q_m) for TiO_2 (68.823 mg/g) and TiO_2@UiO-66-NH_2 (68.729 mg/g). However, the higher Langmuir constant (K_L) and lower separation factor (R_L) for TiO_2 suggest stronger adsorption affinity and more favorable adsorption conditions compared to TiO_2@UiO-66-NH_2. The excellent R^2 value for TiO_2@UiO-66-NH_2 (0.987) indicates a better fit of this model to the composite, implying significant monolayer adsorption (Pourhakkak et al., 2021; C. Wang et al., 2022)

The Freundlich model, which accounts for adsorption on heterogeneous surfaces, highlighted the superior performance of TiO_2@UiO-66-NH_2, with higher K_f (3.383) and n^{-1} (1.218) values compared to TiO_2. These parameters indicate greater adsorption capacity and intensity for the composite. The R^2 value for TiO_2@UiO-66-NH_2 (0.989) further confirms its strong agreement with this model, suggesting multilayer adsorption on a heterogeneous surface, complementing the findings of the Langmuir model.

The Temkin model, which incorporates adsorbate-adsorbent interactions, revealed a higher adsorption energy (b_T) and equilibrium binding constant (K_T) for TiO_2@UiO-66-NH_2 (25.665 J/mol and 81.077 L/mg), demonstrating stronger interactions and better performance compared to TiO_2. However, the moderate R^2 value for TiO_2@UiO-66-NH_2 (0.898) suggests that additional mechanisms may contribute to the adsorption process.

The Dubinin-Radushkevich model provided further insights into the adsorption mechanism. The significantly higher saturation capacity (Q_s) of TiO_2@UiO-66-NH_2 (148.324 mg/g) compared to TiO_2 (58.291 mg/g) confirms its enhanced adsorption potential. The mean adsorption energy (E) for TiO_2 (26.919 kJ/mol) suggests chemisorption, while the lower E value for TiO_2@UiO-66-NH_2 (3.835 kJ/mol) indicates the dominance of physisorption. This distinction highlights the different adsorption behaviors of the two materials (J. Wang & Guo, 2020a).

The interconnected findings from these models reveal that the adsorption of NH_3-N on TiO_2@UiO-66-NH_2 involves a combination of monolayer, multilayer, and physisorption mechanisms, while TiO_2 primarily exhibits monolayer adsorption dominated by chemisorption. The enhanced performance of TiO_2@UiO-66-NH_2 is attributed to its heterogeneous surface and the synergistic properties conferred by UiO-66-NH_2. Overall, the adsorption of NH_3-N on TiO_2@UiO-66-NH_2 is best described by the Freundlich and Langmuir models, as evidenced by higher R^2 values, indicating the occurrence of both monolayer and multilayer adsorption on heterogeneous surfaces.

Table 2. Parameters of the isotherm models for NH_3-N

Isotherm models	Parameters	TiO_2	TiO_2@UiO-66-NH_2
Langmuir	Q_m (mg/g)	68.823	68.729
	K_L (L/mg)	0.009	0.0011
	R_L	0.134	0.6637
	R^2	0.831	0.987
Freundlich	K_f	1.405	3.383
	n^{-1}	0.339	1.218
	R^2	0.847	0.989
Temkin	b_T (J/mol)	19.888	25.665
	K_T (L/mg)	0.056	81.077
	R^2	0.775	0.898
Dubinin Radushkevich	Q_s	58.291	148.324
	β (mol^2/kJ^2)	0.0006	0.261
	E (kJ/mol)	26.919	3.835
	R^2	0.535	0.817

3.4 Adsorption kinetics

The adsorption kinetics of NH_3-N on TiO_2 and TiO_2@UiO-66-NH_2 were evaluated using various kinetic models to understand the mechanism and rate-limiting steps involved in the process. These models included pseudo-first order, pseudo-second order, intraparticle diffusion, Elovich, mass transfer, and Bangham's models. The pseudo-first order model, which assumes that the adsorption rate is proportional to the difference between the current amount of adsorbate and its equilibrium concentration, did not fit the data well for either material, with TiO_2 showing an R^2 value of 0.757 and TiO_2@UiO-66-NH_2 showing an even lower R^2 of 0.411 (Revellame et al., 2020). This suggests that the adsorption on both materials does not follow a simple first-order process, possibly due to the presence of heterogeneous adsorption sites or other factors influencing the adsorption rate. The pseudo-second order model, which is based on chemisorption, where adsorption involves electron sharing or valency forces between the adsorbate and adsorbent, provided a much better fit for both materials, with high R^2 values (0.989 for TiO_2 and 0.997 for TiO_2@UiO-66-NH_2). This indicates that the adsorption of NH_3-N on both TiO_2 and TiO_2@UiO-66-NH_2 is mainly governed by chemisorption. The higher rate constant (K_2) for TiO_2@UiO-66-NH_2 (0.074) compared to TiO_2 (0.0131) suggests that NH_3-N adsorption is faster on the composite material, highlighting the enhanced adsorption capacity of TiO_2@UiO-66-NH_2 (J. Wang & Guo, 2020b)

Intraparticle diffusion, which accounts for the diffusion of the adsorbate within the adsorbent material, did not emerge as the dominant rate-limiting step, as reflected by the relatively low R^2 values for both TiO_2 (0.519) and TiO_2@UiO-66-NH_2 (0.386). The intraparticle diffusion rate constant (K_i)was higher for TiO_2 (0.075) than for TiO_2@UiO-66-NH_2 (0.025), suggesting that diffusion within the TiO_2 particles plays a more significant role in the adsorption

process (Pholosi et al., 2020). The Elovich model, which is often used for heterogeneous surfaces, also showed a good fit for both materials with R^2 values of 0.979 for TiO_2 and 0.935 for TiO_2@UiO-66-NH_2. The rate constant (K) for TiO_2 was significantly higher (1.723) than for TiO_2@UiO-66-NH_2 (0.628), indicating that TiO_2 adsorbs NH_3-N more effectively than the composite. The equilibrium adsorption capacities (Q_e) were 4.2 mg/g for TiO_2 and 1.217 mg/g for TiO_2@UiO-66-NH_2, further confirming the faster adsorption kinetics of TiO_2. The mass transfer model, which describes the diffusion of NH_3-N from the bulk solution to the adsorbent surface, provided valuable insights into the efficiency of adsorption. The mass transfer coefficient (K_0) was much higher for TiO_2@UiO-66-NH_2 (1.806 min^{-1}) compared to TiO_2 (0.152 min^{-1}), indicating that mass transfer is more efficient for the composite material. Both materials showed high R^2 values (0.982 for TiO_2 and 0.977 for TiO_2@UiO-66-NH_2), suggesting that mass transfer plays an important role in the adsorption process. Bangham's model, which focuses on surface diffusion, showed that TiO_2 had a higher surface diffusion coefficient (k_b) of 0.152 L/g compared to TiO_2@UiO-66-NH_2 (0.071 L/g). This indicates that adsorption occurs more efficiently on TiO_2 in terms of surface diffusion, although the fit of the data was moderate with R^2 values of 0.943 for TiO_2 and 0.866 for TiO_2@UiO-66-NH_2 (Largitte & Pasquier, 2016).

In conclusion, the pseudo-second order model provided the best fit for both TiO_2 and TiO_2@UiO-66-NH_2, suggesting that chemisorption is the predominant mechanism governing NH_3-N adsorption. TiO_2 exhibited faster adsorption kinetics, while TiO_2@UiO-66-NH_2 demonstrated superior adsorption capacity, likely due to the enhanced properties of the composite material. These findings suggest that TiO_2@UiO-66-NH_2 may be more suitable for applications where high adsorption capacity is critical, whereas TiO_2 may be more effective in systems requiring rapid adsorption. Further studies on the stability and long-term performance of these materials will be important for their potential application in wastewater treatment.

Table 3. Parameters of the kinetic models for NH_3-N

Kinetic Models	Parameter	TiO_2	TiO_2@UiO-66-NH_2
Pseudo-first order	K_1 (min^{-1})	0.018	0.003
	Q_e (mg/g)	7.047	9.469
	R^2	0.757	0.411
Pseudo-second order	K_2	0.0131	0.074
	Q_e (mg/g)	9.163	3.267
	R^2	0.989	0.997
Intraparticle diffusion	K_i	0.075	0.025
	C_i	3.560	1.494
	R^2	0.519	0.386
Elovich	K	1.723	0.628
	Q_t	4.2	1.217
	R^2	0.979	0.935
Mass transfer	K_0 (min^{-1})	0.152	1.806
	D (mg/L)	6.733	13.985
	R^2	0.982	0.977
Bangham's	k_b (L/g)	0.152	0.071
	R^2	0.943	0.866

4. Conclusions

The TiO_2/UiO-66-NH_2 composites demonstrate significant potential for effectively treating pollutants in produced water. The adsorption behavior aligns with both the Freundlich and Langmuir isotherms. The composites demonstrated impressive removal efficiencies, achieving 88.46% for NH_3-N and 81.97% for TDS, underscoring their effectiveness in addressing common contaminants in produced water. UV-vis analysis revealed a reduced band gap of 2.28 eV for the TiO_2/UiO-66-NH_2 composites, which enhances their ability to absorb visible light and improve photocatalytic performance. Furthermore, the pseudo-second-order kinetic model was the best fit for both TiO_2 and TiO_2@UiO-66-NH_2 composites, indicating that chemisorption is the dominant mechanism for NH_3-N removal. This suggests that the composites exhibit a strong affinity for NH_3-N. Overall, these findings highlight the TiO_2/UiO-66-NH_2 composites as a highly efficient material for mitigating water contamination, with significant potential for applications in both environmental and industrial water treatment processes.

Acknowledgement

The authors would thank to Department of Chemical Engineering, Diponegoro University for the supporting laboratory and facilities.

References

Akinyemi, A., Agboola, O., Alagbe, E., & Igbokwe, E. (2024). The role of catalyst in the adsorption of dye: Homogeneous catalyst, heterogeneous catalyst, and advanced catalytic activated carbon, critical review. *Desalination and Water Treatment*, *320*, 100780. https://doi.org/10.1016/J.DWT.2024.100780

César, S. D., De Jager, D., & Njoya, M. (2024). The role of hydrocyclone and induced gas flotation technologies in offshore produced water deoiling advancements. *Petroleum Research*. https://doi.org/10.1016/J.PTLRS.2024.10.002

Chakravorty, A., & Roy, S. (2024). A review of photocatalysis, basic principles, processes, and materials. *Sustainable Chemistry for the Environment*, *8*, 100155. https://doi.org/10.1016/J.SCENV.2024.100155

Chen, C., Li, X., Zou, W., Wan, H., Dong, L., & Guan, G. (2021). Structural modulation of UiO-66-NH2 metal-organic framework via interligands cross-linking: Cooperative effects of pore diameter and amide group on selective CO2 separation. *Applied Surface Science*, *553*, 149547. https://doi.org/10.1016/J.APSUSC.2021.149547

David, L. O., Nwulu, N., Aigbavboa, C., & Adepoju, O. (2023). Towards global water security: The role of cleaner production. *Cleaner Engineering and Technology*, *17*, 100695. https://doi.org/10.1016/J.CLET.2023.100695

Etacheri, V., Di Valentin, C., Schneider, J., Bahnemann, D., & Pillai, S. C. (2015). Visible-light activation of TiO2 photocatalysts: Advances in theory and experiments.

Journal of Photochemistry and Photobiology C: Photochemistry Reviews, *25*, 1–29. https://doi.org/10.1016/J.JPHOTOCHEMREV.2015.08.003

Farnan, J., Vanden Heuvel, J. P., Dorman, F. L., Warner, N. R., & Burgos, W. D. (2023). Toxicity and chemical composition of commercial road palliatives versus oil and gas produced waters. *Environmental Pollution*, *334*, 122184. https://doi.org/10.1016/J.ENVPOL.2023.122184

Hachemi, C., Abdelmalek, F., Benidris, E. B., Bendahman, R., Andersen, H. R., & Addou, A. (2024). Photocatalytic Fenton-like degradation of Acid Green 25 by novel aluminum nanoferrites with persulfate: Optimization by response surface methodology. *Journal of Alloys and Compounds*, *1009*, 176909. https://doi.org/10.1016/J.JALLCOM.2024.176909

Khan, H., & Shah, M. U. H. (2023). Modification strategies of TiO2 based photocatalysts for enhanced visible light activity and energy storage ability: A review. *Journal of Environmental Chemical Engineering*, *11*(6), 111532. https://doi.org/10.1016/J.JECE.2023.111532

Kumar, A. V., James, T. K., Fizala, M. B., & Mathew, S. (2024). Photocatalytic applications and synthetic strategies of Ti and Fe-based MOFs. *Inorganica Chimica Acta*, *572*, 122297. https://doi.org/10.1016/J.ICA.2024.122297

Kusworo, T. D., Puspa, M. B., Kumoro, A. C., Sutapa, I. D. A., & Utomo, D. P. (2024). Novel photosensitive La@TiO2 nanocomposite: A breakthrough in visible-light photocatalysis for oil field water treatment. *Case Studies in Chemical and Environmental Engineering*, *10*, 100884. https://doi.org/10.1016/J.CSCEE.2024.100884

Largitte, L., & Pasquier, R. (2016). A review of the kinetics adsorption models and their application to the adsorption of lead by an activated carbon. *Chemical Engineering Research and Design*, *109*, 495–504. https://doi.org/10.1016/J.CHERD.2016.02.006

Lei, Y., Zhu, L., Xu, J., Liu, S., Zeng, Z., Li, X., & Wang, G. (2023). The metal organic framework of UiO-66-NH2 reinforced nanofiltration membrane for highly efficient ion sieving. *Journal of Environmental Chemical Engineering*, *11*(6), 111222. https://doi.org/10.1016/J.JECE.2023.111222

Man, Z., Meng, Y., Lin, X., Dai, X., Wang, L., & Liu, D. (2022). Assembling UiO-66@TiO2 nanocomposites for efficient photocatalytic degradation of dimethyl sulfide. *Chemical Engineering Journal*, *431*, 133952. https://doi.org/10.1016/J.CEJ.2021.133952

Mishra, S., & Sundaram, B. (2023). A review of the photocatalysis process used for wastewater treatment. *Materials Today: Proceedings*. https://doi.org/10.1016/J.MATPR.2023.07.147

Monticone, S., Tufeu, R., Kanaev, A. V., Scolan, E., & Sanchez, C. (2000). Quantum size effect in TiO2 nanoparticles: does it exist? *Applied Surface Science*, *162–163*, 565–570. https://doi.org/10.1016/S0169-4332(00)00251-8

Obaideen, K., Shehata, N., Sayed, E. T., Abdelkareem, M. A., Mahmoud, M. S., & Olabi, A. G. (2022). The role of wastewater treatment in achieving sustainable development goals (SDGs) and sustainability guideline. *Energy Nexus*, *7*, 100112. https://doi.org/10.1016/J.NEXUS.2022.100112

Pelaez, M., Nolan, N. T., Pillai, S. C., Seery, M. K., Falaras, P., Kontos, A. G., Dunlop, P. S. M., Hamilton, J. W. J., Byrne, J. A., O'Shea, K., Entezari, M. H., & Dionysiou, D. D. (2012). A review on the visible light active titanium dioxide photocatalysts for environmental applications. *Applied Catalysis B: Environmental*, *125*, 331–349. https://doi.org/10.1016/J.APCATB.2012.05.036

Pholosi, A., Naidoo, E. B., & Ofomaja, A. E. (2020). Intraparticle diffusion of Cr(VI) through biomass and magnetite coated biomass: A comparative kinetic and diffusion study. *South African Journal of Chemical Engineering*, *32*, 39–55. https://doi.org/10.1016/J.SAJCE.2020.01.005

Pourhakkak, P., Taghizadeh, A., Taghizadeh, M., Ghaedi, M., & Haghdoust, S. (2021). Fundamentals of adsorption technology. *Interface Science and Technology*, *33*, 1–70. https://doi.org/10.1016/B978-0-12-818805-7.00001-1

Revellame, E. D., Fortela, D. L., Sharp, W., Hernandez, R., & Zappi, M. E. (2020). Adsorption kinetic modeling using pseudo-first order and pseudo-second order rate laws: A review. *Cleaner Engineering and Technology*, *1*, 100032. https://doi.org/10.1016/J.CLET.2020.100032

Sadia, S. I., Shishir, M. K. H., Ahmed, S., Aidid, A. R., Islam, M. M., Rana, M. M., Al-Reza, S. M., & Alam, M. A. (2024). Crystallographic biography on nanocrystalline phase of polymorphs titanium dioxide (TiO2): A perspective static review. *South African Journal of Chemical Engineering*, *50*, 51–64. https://doi.org/10.1016/J.SAJCE.2024.07.005

Sun, S., Li, H., & Xu, Z. J. (2018). Impact of Surface Area in Evaluation of Catalyst Activity. *Joule*, *2*(6), 1024–1027. https://doi.org/10.1016/J.JOULE.2018.05.003

Wang, C., Wang, Z., Mao, S., Chen, Z., & Wang, Y. (2022). Coordination environment of active sites and their effect on catalytic performance of heterogeneous catalysts. *Chinese Journal of Catalysis*, *43*(4), 928–955. https://doi.org/10.1016/S1872-2067(21)63924-4

Wang, J., & Guo, X. (2020a). Adsorption isotherm models: Classification, physical meaning, application and solving method. *Chemosphere*, *258*, 127279. https://doi.org/10.1016/J.CHEMOSPHERE.2020.127279

Wang, J., & Guo, X. (2020b). Adsorption kinetic models: Physical meanings, applications, and solving methods. *Journal of Hazardous Materials*, *390*, 122156. https://doi.org/10.1016/J.JHAZMAT.2020.122156

Wang, Y. L., Zhang, S., Zhao, Y. F., Bedia, J., Rodriguez, J. J., & Belver, C. (2021). UiO-66-based metal organic frameworks for the photodegradation of acetaminophen under simulated solar irradiation. *Journal of Environmental Chemical Engineering*, *9*(5), 106087. https://doi.org/10.1016/J.JECE.2021.106087

Ye, L., & Liang, Y. (2024). First principles study on band gap modulation of TiO2 (112) surface for enhancing optical properties. *Physica B: Condensed Matter*, *674*, 415579. https://doi.org/10.1016/J.PHYSB.2023.415579

Zhuang, Y., Ji, Y., Kuang, Q., Zhang, Z., Li, P., Song, J., & He, N. (2023). Oxidation treatment of shale gas produced water: Molecular changes in dissolved organic matter composition and toxicity evaluation. *Journal of Hazardous Materials*, *452*, 131266. https://doi.org/10.1016/J.JHAZMAT.2023.131266